Mechanical properties of bovine articular cartilage under microscale indentation loading from atomic force microscopy

S Park[1]*, **K D Costa**[2], **G A Ateshian**[2,3], and **K-S Hong**[1]
[1]School of Mechanical Engineering, Pusan National University, Busan, Republic of Korea
[2]Department of Biomedical Engineering, Columbia University, New York, USA
[3]Department of Mechanical Engineering, Columbia University, New York, USA

The manuscript was received on 17 September 2008 and was accepted after revision for publication on 16 December 2008.

DOI: 10.1243/09544119JEIM516

Abstract: Atomic force microscopy (AFM) techniques have been increasingly used for investigating the mechanical properties of articular cartilage. According to the previous studies reporting the microscale Young's modulus under AFM indentation tests, the Hertz contact model has been employed with a sharp conical tip indenter. However, the non-linear microscale behaviour of articular cartilage could not be resolved by the standardized Hertz analysis using small and sharp atomic force microscope tips. Therefore, the objective of this study was to evaluate the microscale Young's modulus of articular cartilage more accurately through a non-Hertzian approach with a spherical tip of 5 μm diameter, and to characterize its microscale mechanical behaviour. This methodology adopted in the present study was proved by the consistent values between the microscale (2 per cent, about 9.3 kPa; 3 per cent, about 17.5 kPa) and macroscale (2 per cent, about 8.3 kPa; 3 per cent, about 18.3 kPa) Young's moduli for 2 per cent and 3 per cent agarose gel ($n = 100$). Therefore, the microscale Young's modulus evaluated in this study is representative of more accurate measurements of cartilage stiffness at the 600 nm deformation level and corresponds to approximately 30.9 kPa ($n = 100$). Furthermore, on this level of the microscale deformation, articular cartilage showed depth-dependent and frequency-independent behaviour under AFM indentation loading. These findings reveal the microscale mechanical behaviour of articular cartilage more accurately and can be employed further to design microscale structures of chondrocyte-seeded scaffolds and tissue-engineered cartilage by evaluating their microscale properties.

Keywords: atomic force microscopy, cartilage mechanics, mechanical response, microscale indentation

1 INTRODUCTION

Atomic force microscopy (AFM) techniques have increasingly been used for measuring tribological and mechanical properties (i.e. surface roughness, wear, friction, elastic modulus, and boundary lubrication) of engineering and biological surfaces on nanoscale and microscale levels [**1**–**6**]. AFM tribological studies have been reported on many biological surfaces (hydrogels, phospholipid co-adsorbed layers, dentin, enamel, dentino-enamel junction, and human hair) [**7**–**12**] as well as the cartilage surface [**3**, **13**–**15**]. AFM indentation testing has also been widely used to calculate mechanical properties of soft materials by evaluating the elastic modulus E from the Hertz contact model [**16**–**24**]. However, these AFM indentation studies have been performed on the cells (human umbilical vein endothelial cells, liver epithelial cells, cardiac muscle cells, skeletal muscle cells, etc.) and biological fibres and have mainly focused on the spatial variations in their elastic moduli. By adopting the Hertz contact

Corresponding author: School of Mechanical Engineering, Pusan National University, 30 Jangjeon-dong, Geumjeong-gu, Busan, 609-735, Republic of Korea. email: paks@pusan.ac.kr

model, Mathur *et al.* [**20**] have reported an elastic modulus of about 7.2 kPa over the nucleus, about 3.0 kPa over the cell body in proximity to the nucleus, and about 1.3 kPa on the cell body near the edge. Costa *et al.* [**25**] have adopted a non-Hertzian approach because of the unrealistic assumptions of a simplified Hertz theory and reported the average pointwise moduli of approximately 5.6 kPa and approximately 1.5 kPa for two distinct populations of human aortic endothelial cells at an indentation depth up to 200 nm.

Regarding articular cartilage, the mechanical material properties have not yet been well characterized on microscale levels; neither have the relationships between microscale and macroscale mechanical properties. There are only limited AFM data for articular cartilage. Young's moduli E_Y of rabbit jaw condylar articular cartilage calculated by the Hertz contact model with an oxide-sharpened conical atomic force microscope tip (radius of curvature, about 20 nm) have been compared for neonatal tissue (about 0.9–1.0 MPa) and adult tissue (about 1.0–2.3 MPa) as well as for the anteromedial region (about 2.3 MPa) and the posterolateral region (about 1.0 MPa) [**26**, **27**]. Most AFM studies in the literature have used small and sharp atomic force microscope tips for indentation testing on the soft materials including articular cartilage. Dimitriadis *et al.* [**28**] have shown that the most fundamental assumption of the Hertz contact model, i.e. small deformations or strains, is easily violated by sharp atomic force microscope cantilever tips, but spherical atomic force microscope cantilever tips can reduce the non-linearity of soft materials compared with sharp cantilever tips. These spherical atomic force microscope tips (2.5 μm and 10 μm radius) have been used to measure frictional coefficients of articular cartilage (about 0.15) [**15**], intertubular dentin (about 0.31) and enamel (about 0.14) [**12**] to minimize ploughing forces from plastic deformation. Moreover, the effective compressive modulus E^* of articular cartilage has been measured in a recent study with a spherical atomic force microscope tip (2.5 μm radius) by three of the present authors [**15**] by curve fitting AFM indentation data with the Hertz contact model which gave $E^* \approx 46$ kPa. However, because even the spherical atomic force microscope cantilever tips are not able to resolve the non-linear behaviour of articular cartilage completely on a microscale [**15**], another approach without using the standardized Hertz analysis is desirable to measure the microscale modulus of articular cartilage more accurately.

Therefore, the objective of the present study was to measure the microscale Young's modulus E_Y of articular cartilage more accurately by adopting a non-Hertzian approach [**25**] and using a relatively large spherical atomic force microscope tip. The second objective was to characterize the microscale mechanical response of articular cartilage.

2 MATERIALS AND METHODS

2.1 Sample preparation

Two cylindrical osteochondral plugs (diameter 8 mm, $h = \approx 1.5$ mm) were harvested from two fresh bovine humeral heads (2–4 months old). Using a sledge microtome (model 1400; Leiz, USA), approximately 1 mm of the tissue for AFM was taken from the deep zone to remove remnants of subchondral bone and vascularized tissue and to produce a surface parallel to the articular side, leaving the articular surface intact. Cartilage samples were refrigerated at 4 °C and tested within 3 days, but never frozen. In order to validate the microscale Young's moduli from AFM measurements by comparison with the macroscale Young's moduli, 2 per cent and 3 per cent (wt/vol) low-melt agarose hydrogels (type VII, Sigma Chemicals, USA) were also prepared.

2.2 Microscale AFM indentation experiment

Samples (2 per cent and 3 per cent agarose gel; articular cartilage) for AFM indentation testing were glued on the bony side to 35 mm polystyrene petri dishes using a small amount of cyanoacrylate glue. AFM indentation testing was conducted with samples entirely submerged in phosphate-buffered saline (PBS) on a Bioscope atomic force microscope (Digital Instruments, USA) with Z limits for indentation of 2.5 V and 20 V (Fig. 1). Custom silicon nitride AFM probes with polystyrene spherical tips ($R = 2.5$ μm; Novascan Technologies, USA) having a nominal spring constant of $k = 0.32$ N/m were used for AFM indentation testing. The mounted probe was submerged in PBS for at least 20 min prior to imaging to allow for thermal equilibration at room temperature.

Before AFM indentation testing, the deflection sensitivity was determined in PBS on glass every time that the atomic force microscope cantilever probe was mounted on the atomic force microscope head, and it ranged from 41.17 nm/V to 63.86 nm/V. Approach signals from AFM indentation tests were

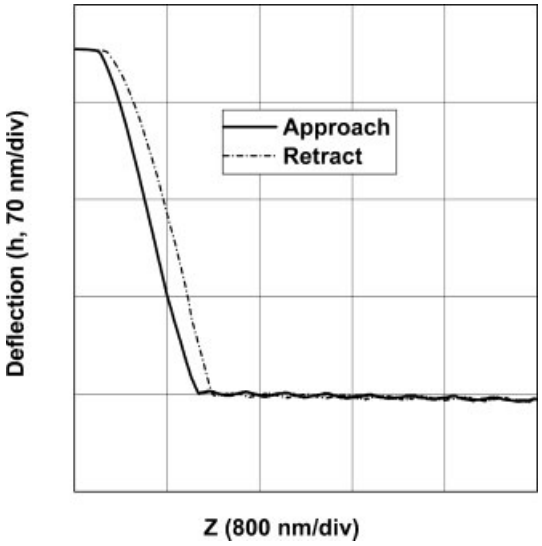

Fig. 1 Typical profile of the approaching and retracting signals of AFM indentation loading on the surface of articular cartilage at 9.3 Hz loading frequency with a Z limit of 20 V

cantilever normal deflection h signals as a function of sample position height Z produced by Nanoscope III software obtained with the AFM device (Digital Instruments, USA). These approach signals were converted to the indentation depth $D = Z - h$ versus indentation load $F = kh$ curves (Fig. 2). Because the indentation depth D_i and load F_i of the ith data point were assumed to be related by the Hertz contact formula $F_i = \frac{4}{3}E_i^* R_i^{1/2} D_i^{3/2}$, the pointwise effective moduli E_i^* of each data point i for the indentation depth–load data were calculated by an equation of the form $E_i^* = F_i \Big/ \left(\frac{4}{3}E_i^* R_i^{1/2} D_i^{3/2}\right)$ with $R = 2.5\,\mu$m as shown in Figs 3, 4, and 5 [**17**, **23**, **25**, **29**, **30**]. These pointwise effective moduli E_i^* of each data point i were averaged over all data points of the indentation depth–load curve to obtain an average pointwise E^* over the indentation depth $D = 300$ nm (Z limit, 2.5 V) and $D = 600$ nm (Z limit, 20 V), instead of performing a least-squares fit of the measured indentation depth–load data with the Hertz contact formula to extract a single value of E^* from each indentation curve. The average pointwise effective modulus E^* over the indentation depth for each AFM measurement was converted to the average pointwise Young's modulus (i.e. the microscale E_Y) from the equation $E^* = E_Y/(1 - \nu^2)$ where Poisson's ratio $\nu = 0.5$ [**17**, **23**, **25**, **29**, **30**]. To identify the ideal contact point between the atomic force microscope tip and the sample surface, a two-part polynomial model-fitting algorithm developed by Costa *et al.* [**25**] was adopted.

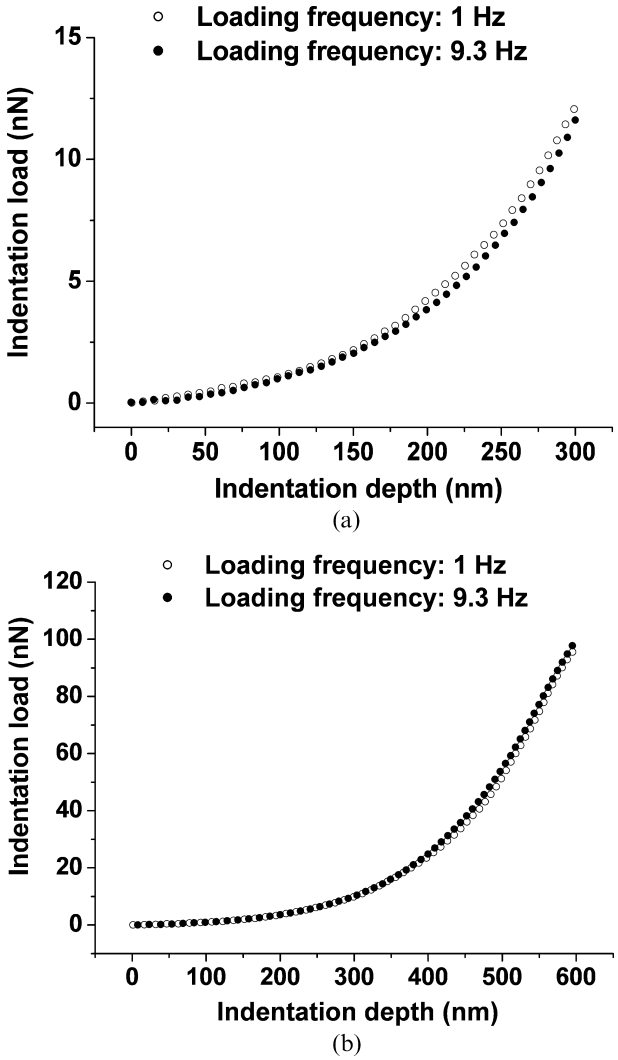

Fig. 2 Typical profiles of cartilage indentation depth versus indentation load which were converted from the approaching signal of AFM indentation with the indentation depths of (a) up to 300 nm and (b) up to 600 nm

2.3 Microscale E_Y of agarose gel and articular cartilage

AFM indentation tests were performed on each 2 per cent and 3 per cent (wt/vol) agarose hydrogel with a Z limit of 20 V at 1 Hz loading frequency. The microscale E_Y (i.e. the average pointwise E_Y) over the indentation depth of 600 nm for each indentation depth–force curve was calculated from the pointwise E^* (Fig. 5) using the method explained above in order to compare these microscale E_Y values of 2 per cent and 3 per cent agarose gels with their macroscale E_Y values. The same experimental method was used for the cartilage samples, and then the microscale E_Y of articular cartilage was obtained ($n = 100$).

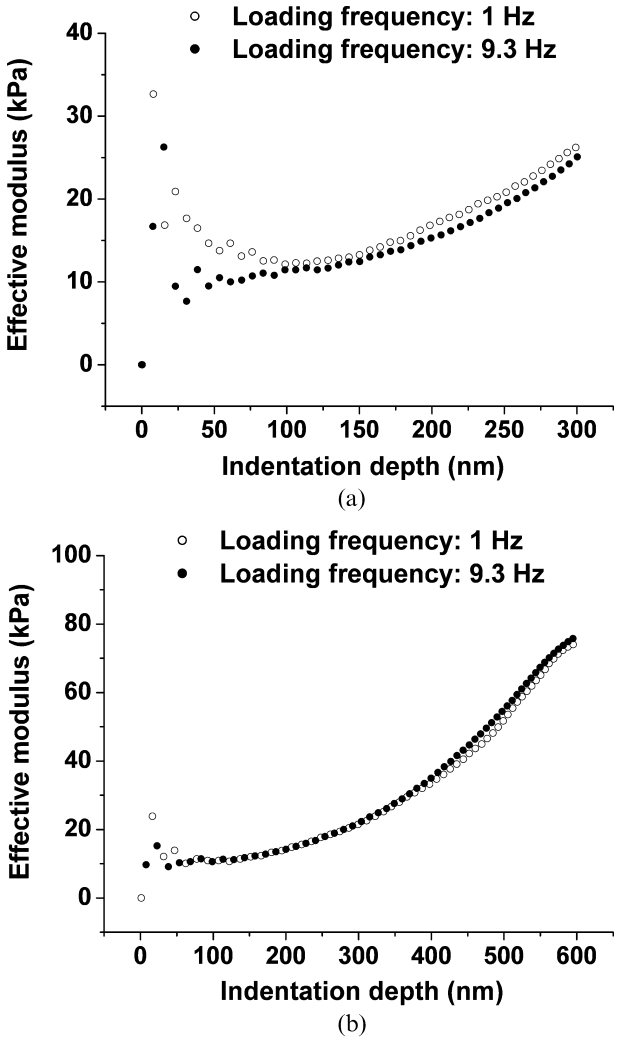

Fig. 3 Pointwise effective modulus $E^* = E_Y/(1-\nu^2)$ of articular cartilage as a function of indentation depth, calculated at each data point of the indentation depth versus indentation load curve with the indentation depths of (a) up to 300 nm and (b) up to 600 nm

2.4 Microscale mechanical response of articular cartilage

AFM indentation tests were performed on the cartilage sample with Z limits of 2.5 V and 20 V at 1 Hz and 9.3 Hz loading frequencies. The microscale E_Y was also calculated for each indentation curve using the same method explained above over the indentation depths up to $D = 300$ nm (Z limit, 2.5 V) and $D = 600$ nm (Z limit, 20 V) at 1 Hz and 9.3 Hz loading frequencies.

2.5 Macroscale unconfined compression experiment (macroscale E_Y of agarose gel)

The custom-designed testing apparatus consisted of a voice-coil force actuator (model LA17-28-000A; BEI Kimco Magnetics Division, USA; 71 N peak force), connected in series with a linear variable-differential transformer for displacement measurements (model PR812-200, Schaeviz Sensors, USA; ± 5 mm), a loading platen consisting of glass 1 mm thick, the tissue sample, and a stainless steel specimen chamber mounted on a load cell (model 8523, Burster, USA; ± 200 N). The force actuator, connected to a power supply (model PST-040-13-DP, Copley Controls Corp., USA; +40 V d.c. at 13 A continuous) and controller box (model TA115, Trust Automation INC., USA; 150 W continuous, 325 W peak) was controlled via a force feedback loop using a desktop computer with a data input and output board (model PCI-MIO-16XE-10, National Instruments, USA) running the LabView software package (version 6.1, National Instruments, USA).

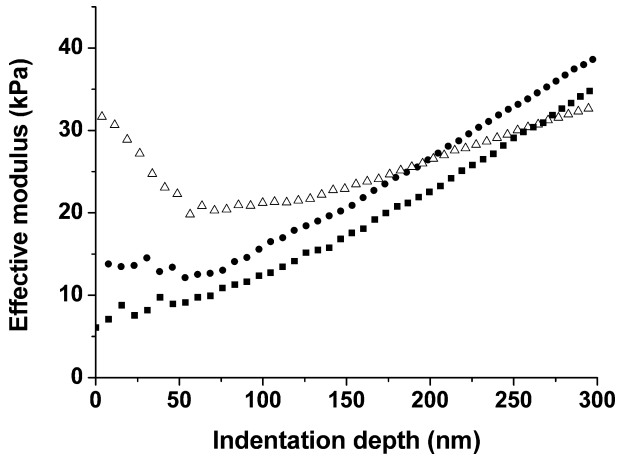

Fig. 4 Initial behaviour of the pointwise effective modulus E^* categorized by three types of response (depth-dependent initial increase, decrease, and initially almost depth-independent constant response) from AFM indentation measurements on articular cartilage with an indentation depth of up to 300 nm at 1 Hz loading frequency

2 per cent and 3 per cent agarose gels (diameter 8 mm; $h = 1.4$ mm) were mounted on a PBS-filled testing chamber, and the specimen was allowed to equilibrate for 4.4 h under a tare load of 0.2 N (equivalent to 4.0 kPa). The reductions in thickness resulting from tare load application were 47.9 per cent for 2 per cent agarose gel and 21.8 per cent for 3 per cent agarose gel. The macroscale E_Y values of 2 per cent and 3 per cent agarose gels were determined from the applied tare load divided by the reduction in thickness.

2.6 Statistical analyses

One-way analysis of variance (ANOVA) was performed to investigate statistical differences between

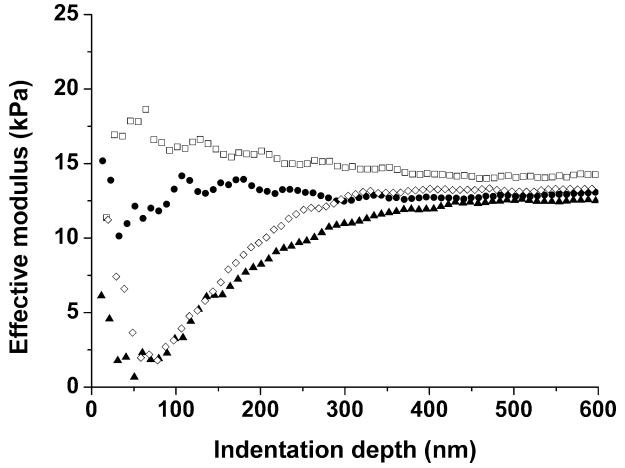

Fig. 5 Pointwise effective modulus E^* of 2 per cent agarose gel reaching an equilibrium value after the depth-dependent and/or almost depth-independent initial behaviours (indentation depth, 600 nm; loading frequency, 1 Hz)

the microscale E_Y values of 2 per cent and 3 per cent agarose gels (SAS Institute Inc., USA). Similarly, two-way ANOVA with repeated measures was used to investigate the effects of indentation depths (300 nm and 600 nm) and loading frequencies (1 Hz and 9.3 Hz) on the microscale E_Y of articular cartilage; post-hoc testing of the means was performed with Bonferroni adjustment [**31**, **32**]. In all cases, α was set at 0.05 and the significance was set at $p < 0.05$.

3 RESULTS

The microscale Young's moduli E_Y of 2 per cent and 3 per cent agarose gels up to 600 nm indentation depth at 1 Hz loading frequency were 9.3 ± 2.3 kPa ($n = 100$) and 17.5 ± 3.0 kPa ($n = 100$) respectively, and similar to their macroscale E_Y values (2 per cent agarose gel, 8.3 kPa; 3 per cent agarose gel, 18.3 kPa). 3 per cent agarose gel was much stiffer than 2 per cent agarose gel based on the statistical differences in the microscale E_Y values ($p < 0.001$). It was found that the microscale E_Y values of articular cartilage calculated from AFM indentation tests under the same loading conditions were 30.9 ± 14.3 kPa ($n = 100$).

The pointwise elastic modulus E^* of agarose gel reached equilibrium values (Fig. 5), while the pointwise E^* of articular cartilage showed a non-linear increase with an increase in the indentation depth (Fig. 3) after three typical types of the depth-dependent and/or depth-independent initial behaviours (depth-dependent initial increase and decrease, and initially almost depth-independent constant response) (Fig. 4).

A two-way ANOVA for the factors of indentation loading frequency and indentation depth shows that the microscale E_Y of articular cartilage increases significantly with an increase in the applied indentation depth at both 1 Hz and 9.3 Hz loading frequencies ($p < 0.001$) (Fig. 3); the indentation depth-dependent E_Y increased from 16.4 ± 6.5 kPa to 30.9 ± 13.5 kPa at 1 Hz loading frequency and from 14.9 ± 6.2 kPa to 32.6 ± 10.3 kPa at 9.3 Hz loading frequency ($n = 12$) when the indentation depth increased from 300 nm to 600 nm. However, the effect of loading frequency on the microscale E_Y of articular cartilage was not significant; the microscale E_Y values at 1 Hz and 9.3 Hz loading frequencies exhibited no statistical differences ($p = 1.0$) (Fig. 3).

4 DISCUSSION

The main objective of the present study was to evaluate a more accurate microscale Young's modulus E_Y of articular cartilage. Experimentally, this was achieved by AFM indentation tests through a non-Hertzian approach [**25**] with a relatively large spherical atomic force microscope tip. The result that the microscale E_Y values of 2 per cent and 3 per cent agarose gels (about 9.3 kPa and about 17.5 kPa respectively) are similar to the macroscale E_Y values of 2 per cent and 3 per cent agarose gels (about 8.3 kPa and about 18.3 kPa respectively) supports accurate measurements of the microscale E_Y values. The microscale E_Y of articular cartilage evaluated from this AFM technique was approximately 30.9 kPa. This value may seem to be relatively small when compared with the macroscale E_Y of bovine cartilage. However, when the depth-dependent inhomogeneous behaviour of articular cartilage is considered, the microscale E_Y is in good agreement with the macroscale E_Y of articular cartilage. On a macroscale, E_Y has been reported to be about 490 kPa when bovine cartilage was compressed by a deformation of about 200 μm from approximately 1.83 mm thickness [**33**]. This depth-dependent E_Y has further decreased to about 100 kPa when investigated within 5 per cent of the full-thickness depth from the articular surface under an average tissue compressive strain of 10 per cent by optical measurements methods and digital image analysis [**34**, **35**]. Accounting for the magnitude of the 600 nm indentation depth of this study, it seems reasonable to conclude that AFM measurements of E_Y at the ultrathin surface layer of articular cartilage are

consistent with these previous findings. However, this conclusion is based on comparisons between the microscale E_Y of the current study obtained from unfrozen samples and the macroscale E_Y of the literature calculated from frozen samples. Although the previous study has shown that freezing of articular cartilage for 24 h has no significant effect on microscale surface roughness and superficial structure, it will be important to measure directly the effect of the freezing period of articular cartilage on the microscale E_Y as well as its relationships with the surface roughness and superficial structure of articular cartilage.

From the theoretical analysis of articular cartilage based on the biphasic theory [**36**], the characteristic time constant $\tau = a^2/H_A k$ on the macroscale which explains the time-dependent decrease in interstitial fluid load support of articular cartilage [**37–39**] yields 2051 s using the representative material properties of immature bovine cartilage from a previous study by two of the present anthors [**40**], where the radius of the contact area is $a = 4$ mm, the aggregate tensile modulus of the solid matrix is $H_A = 13$ MPa, and the hydraulic permeability is $k = 0.6 \times 10^{-15}$ m^4/N s. On a microscale, however, because of the very small size of the atomic force microscope indenter tip, $a = 2.5$ μm, the time constant is equal to 0.8 ms. Consequently, interstitial fluid pressurization will subside very rapidly in AFM indentation measurements with applied loading frequencies of 1 Hz and 9.3 Hz, and the microscale E_Y of articular cartilage of this study corresponds to the intrinsic (fluid-independent) property of cartilage solid phase independently of the effect of its fluid phase.

This study was also aimed at characterizing the microscale mechanical response of articular cartilage by applying microscale strains ranged within the regions of lamina splendens (the ultrathin layer of the articular surface within 5–10 μm) of articular cartilage. On a macroscale, a previous study by two of the present authors and a co-worker [**33**] has reported that fluid-dependent viscoelasticity and non-linearity of articular cartilage play an important role in providing cartilage with the functional properties that allow it to sustain the severe loading environment in joints. However, in this study, calculation of the pointwise E^* at each data point of the AFM indentation depth–force curve was performed under the assumption that the microscale behaviour of articular cartilage would be elastic, and the result that the microscale E_Y values at 1 Hz and 9.3 Hz loading frequencies were not significantly different did not contradict this elastic assumption of articular cartilage for a microscale deformation of less than 600 nm.

Another important finding of this study was that statistically significant differences between the microscale E_Y values of articular cartilage calculated by averaging its pointwise E^* over the indentation depths of either 300 nm or 600 nm were observed between these two deformation levels (300 nm and 600 nm). This observation of the indentation depth-dependent cartilage microscale E_Y is consistent with the macroscale inhomogeneous behaviour of articular cartilage [**33**, **41**]. According to the study by Krishnan *et al.* [**41**], the assumption of an inhomogeneous cartilage layer to loading shows more increase in the interstitial fluid load support than the homogeneous assumption and results in the enhancement of the friction and wear properties of articular cartilage from finite element method on a macroscale. While new information on the microscale mechanical properties of articular cartilage has been provided from this study, it is important to outline the limitations of this study. Although 100 AFM indentation measurements of the microscale E_Y values for 2 per cent and 3 per cent agarose gels were performed, no statistical analysis between the microscale and macroscale E_Y values was conducted because only one measurement of the macroscale E_Y values for 2 per cent and 3 per cent agarose gels was performed with the assumption of consistent macroscale behaviour for agarose gel based on its homogeneous structure, which is a limitation of this study. Another limitation of this study is that different selections of the initial contact points between the atomic force microscope tip and sample surface from even the same approaching signal of AFM indentation loading affect the initial behaviour of the pointwise E^* of articular cartilage (Fig. 6). Although the ideal contact points between the atomic force microscope tip and cartilage surface were determined by employing a two-part polynomial model-fitting algorithm of the literature in order to minimize the examiner's subjective judgements [**25**], the initial responses of the pointwise E^* values were not consistently the same, showing three types of behaviour (depth-dependent initial increase and decrease, and initially an almost depth-independent constant response) (Fig. 4). Because the initial depth-dependent decrease in the pointwise E^* of articular cartilage is clearly different from its overall depth-dependent increase (i.e. statistically significant differences between the average values of the pointwise E^* over 300 nm and 600 nm indentation depths), it is a limitation of this study caused by the

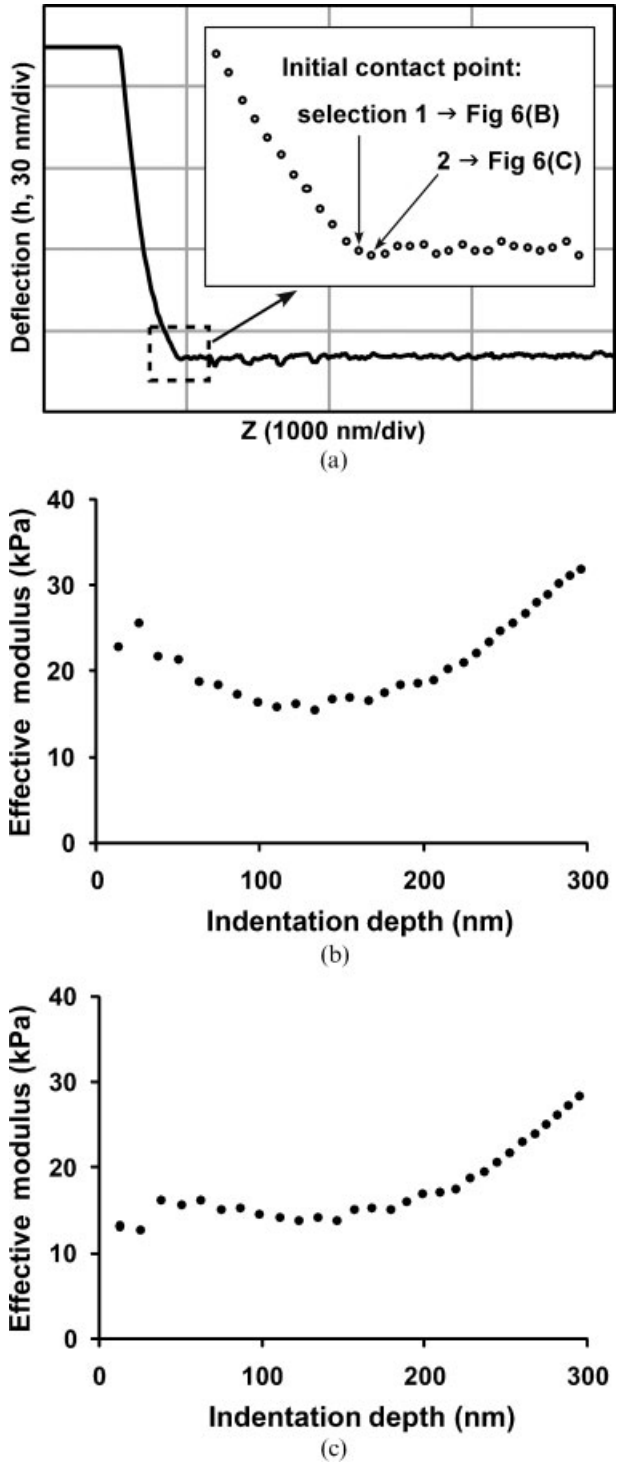

Fig. 6 (a) Different selections (selections 1 and 2) of the initial contact points between the atomic force microscope tip and sample surface from the same approaching signal of AFM indentation loading (indentation depth, 300 nm; loading frequency, 1 Hz) which affect the initial behaviour of the pointwise effective modulus E^* of articular cartilage. (b) Depth-dependent initial decrease and then increase for selection 1 of the contact point. (c) Almost depth-independent constant initial response for selection 2 of the contact point

dependence on the selections of the initial contact points between the atomic force microscope tip and sample surface from AFM indentation data. However, it is believed that this limitation could be overcome to some extent by the averaging method of the pointwise E^* values over the indentation depth of 300 nm and/or 600 nm to calculate the microscale E_Y.

In summary, this study reports more accurate measurements of the microscale mechanical response of articular cartilage from AFM indentation which can be adopted for assessing microscale mechanical properties in tissue-engineered cartilage and designing microscale structures of chondrocytes-seeded scaffolds. In future studies, it is planned to use the experimental results of this study to formulate a constitutive relation which accounts for the observed depth-dependent and frequency-independent behaviour on a microscale, and further to extend to the investigation the effect of cytokines (i.e. IL-1 and TNF-α) on the microscale properties of chondrocytes and collagen fibrils of articular cartilage.

ACKNOWLEDGEMENTS

This study was supported by funds from the National Institute of Arthritis and Musculoskeletal and Skin Diseases of the National Institutes of Health (AR-46532, AR-43628) and by the Korea Research Foundation Grant funded by the Korean Government (Basic Research Promotion Fund of the Ministry of Education and Human Resources Development grant KRF-2007-331-D00593).

REFERENCES

1 **Bhushan, B.** *Handbook of micro/nanotribology*, 1995 (CRC Press, Boca Raton, Florida).
2 **Bhushan, B.** Micro/nanotribology using atomic force microscopy/friction force microscopy: state of the art. *Proc. Instn Mech. Engrs, Part J: J. Engineering Tribology*, 1995, **212**(1), 1–18.
3 **Kumar, P., Oka, M., Toguchida, J., Kobayashi, M., Uchida, E., Nakamura, T.,** and **Tanaka, K.** Role of uppermost superficial surface layer of articular cartilage in the lubrication mechanism of joints. *J. Anat.*, 2001, **199**, 241–250.
4 **Du, B. Y., VanLandingham, M. R., Zhang, Q. L.,** and **He, T. B.** Direct measurement of plowing friction and wear of a polymer thin film using the atomic force microscope. *J. Mater. Res.*, 2001, **16**(5), 1487–1492.
5 **Bhushan, B.** and **Koinkar, V. N.** Nanoscale boundary lubrication studies using AFM/FFM. *Abstr. Papers Am. Chem. Soc.*, 1996, **212**, 239-Poly.

6 **Kim, J. H., Lee, H. K., Choi, B. I., Kang, J. Y.,** and **Oh, C. S.** Mechanical property measurement in nano imprint process. *J. Korean Soc. Precision Engng*, 2004, **21**(6), 7–14.

7 **Kim, S. H., Marmo, C.,** and **Somorjai, G. A.** Friction studies of hydrogel contact lenses using AFM: non-crosslinked polymers of low friction at the surface. *Biomaterials*, 2001, **22**(24), 3285–3294.

8 **Kim, S. H., Opdahl, A., Marmo, C.,** and **Somorjai, G. A.** AFM and SFG studies of pHEMA-based hydrogel contact lens surfaces in saline solution: adhesion, friction, and the presence of non-crosslinked polymer chains at the surface. *Biomaterials*, 2002, **23**(7), 1657–1666.

9 **Gong, J. P., Iwasaki, Y., Osada, Y., Kurihara, K.,** and **Hamai, Y.** Friction of gels. 3. Friction on solid surfaces. *J. Phys. Chemistry B*, 1999, **103**(29), 6001–6006.

10 **Grant, L. M.** and **Tiberg, F.** Normal and lateral forces between lipid covered solids in solution: correlation with layer packing and structure. *Biophys. J*, 2002, **82**(3), 1373–1385.

11 **McMullen, R. L.** and **Kelty, S. P.** Investigation of human hair fibers using lateral force microscopy. *Scanning*, 2001, **23**(5), 337–345.

12 **Habelitz, S., Marshall, S. J., Marshall Jr, G. W.,** and **Balooch, M.** The functional width of the dentino-enamel junction determined by AFM-based nano-scratching. *J. Struct. Biology*, 2001, **135**(3), 294–301.

13 **Jurvelin, J. S., Muller, D. J., Wong, M., Studer, D., Engel, A.,** and **Hunziker, E. B.** Surface and subsurface morphology of bovine humeral articular cartilage as assessed by atomic force and transmission electron microscopy. *J. Struct. Biology*, 1996, **117**(1), 45–54.

14 **Moa-Anderson, B. J., Costa, K. D., Hung, C. T.,** and **Ateshian, G. A.** Bovine articular cartilage surface topography and roughness in fresh versus frozen tissue samples using atomic force microscopy. In Proceedings of 2003 Summer Bioengineering Conference, Key Biscayne, Florida, USA, 25–29 June 2003, p. 0561 (ASME International, New York).

15 **Park, S., Costa, K. D.,** and **Ateshian, G. A.** Microscale frictional response of bovine articular cartilage from atomic force microscopy. *J. Biomechanics*, 2004, **37**(11), 1679–1687.

16 **A-Hassan, E., Heinz, W. F., Antonik, M. D., D'Costa, N. P., Nageswaran, S., Schoenenberger, C. A.,** and **Hoh, J. H.** Relative microelastic mapping of living cells by atomic force microscopy. *Biophys. J.*, 1998, **74**(3), 1564–1578.

17 **Costa, K. D.** and **Yin, F. C. P.** Analysis of indentation: implications for measuring mechanical properties with atomic force microscopy. *Trans. ASME, J. Biomech. Engng*, 1999, **121**(5), 462–471.

18 **Heinz, W. F.** and **Hoh, J. H.** Spatially resolved force spectroscopy of biological surfaces using the atomic force microscope. *Trends Biotechnol.*, 1999, **17**(4), 143–150.

19 **Parbhu, A. N., Bryson, W. G.,** and **Lal, R.** Disulfide bonds in the outer layer of keratin fibers confer higher mechanical rigidity: correlative nano-indentation and elasticity measurement with an AFM. *Biochemistry*, 1999, **38**(36), 11 755–11 761.

20 **Mathur, A. B., Truskey, G. A.,** and **Reichert, W. M.** Atomic force and total internal reflection fluorescence microscopy for the study of force transmission in endothelial cells. *Biophys. J.*, 2000, **78**(4), 1725–1735.

21 **Mathur, A. B., Collinsworth, A. M., Reichert, W. M., Kraus, W. E.,** and **Truskey, G. A.** Endothelial, cardiac muscle and skeletal muscle exhibit different viscous and elastic properties as determined by atomic force microscopy. *J. Biomechanics*, 2001, **34**(12), 1545–1553.

22 **Collinsworth, A. M., Zhang, S., Kraus, W. E.,** and **Truskey, G. A.** Apparent elastic modulus and hysteresis of skeletal muscle cells throughout differentiation. *Am. J. Physiology, Cell Physiology*, 2002, **283**(4), C1219–C1227.

23 **Radmacher, M.** Measuring the elastic properties of living cells by the atomic force microscope. In *Atomic force microscopy in cell biology* (Eds B. P. Jena and J. K. Horber), 2002, pp. 67–90 (Academic Press, New York).

24 **Braet, F., Rotsch, C., Wisse, E.,** and **Radmacher, M.** Comparison of fixed and living liver endothelial cells by atomic force microscopy. *Appl. Physics A: Mater. Sci. Processing*, 1998, **66**, S575–S578.

25 **Costa, K. D., Sim, A. J.,** and **Yin, F. C.** Non-Hertzian approach to analyzing mechanical properties of endothelial cells probed by atomic force microscopy. *Trans. ASME, J. Biomech. Engng*, 2006, **128**(2), 176–184.

26 **Patel, R. V.** and **Mao, J. J.** Microstructural and elastic properties of the extracellular matrices of the superficial zone of neonatal articular cartilage by atomic force microscopy. *Frontiers Biosci.*, 2003, **8**, A18–A25.

27 **Hu, K., Radhakrishnan, P., Patel, R. V.,** and **Mao, J. J.** Regional structural and viscoelastic properties of fibrocartilage upon dynamic nanoindentation of the articular condyle. *J. Struct. Biol.*, 2001, **136**(1), 46–52.

28 **Dimitriadis, E. K., Horkay, F., Maresca, J., Kachar, B.,** and **Chadwick, R. S.** Determination of elastic moduli of thin layers of soft material using the atomic force microscope. *Biophysi. J.*, 2002, **82**(5), 2798–2810.

29 **Johnson, K. L.** *Contact mechanics*, 1985 (Cambridge University Press, Cambridge).

30 **Costa, K. D.** Imaging and probing cell mechanical properties with the atomic force microscope. *Meth. Molecular Biology*, 2006, **319**, 331–361.

31 **Miller, R. G.** *Simultaneous statistical inference*, 1981 (Springer-Verlag, New York).

32 **Dewey, M. E.** Bonferroni. In *Encyclopedia of biostatistics* (Eds P. Armitage and T. Colton), 2005, pp. 420–421 (John Wiley, Chichester, West Sussex).

33 **Park, S., Hung, C. T.,** and **Ateshian, G. A.** Mechanical response of bovine articular cartilage under dynamic unconfined compression loading at physiological stress levels. *Osteoarthritis Cartilage*, 2004, **12**(1), 65–73.

34 **Schinagl, R. M., Gurskis, D., Chen, A. C.,** and **Sah, R. L.** Depth-dependent confined compression modulus of full-thickness bovine articular cartilage. *J. Orthop. Res.*, 1997, **15**(4), 499–506.

35 **Wang, C. C., Deng, J. M., Ateshian, G. A.,** and **Hung, C. T.** An automated approach for direct measurement of two-dimensional strain distributions within articular cartilage under unconfined compression. *Trans. ASME, J. Biomech. Engng*, 2002, **124**(5), 557–567.

36 **Mow, V. C., Kuei, S. C., Lai, W. M.,** and **Armstrong, C. G.** Biphasic creep and stress relaxation of articular cartilage in compression? Theory and experiments. *Trans. ASME, J. Biomech. Engng*, 1980, **102**(1), 73–84.

37 **Armstrong, C. G., Lai, W. M.,** and **Mow, V. C.** An analysis of the unconfined compression of articular cartilage. *Trans. ASME, J. Biomech. Engng*, 1984, **106**(2), 165–173.

38 **Ateshian, G. A., Lai, W. M., Zhu, W. B.,** and **Mow, V. C.** An asymptotic solution for the contact of two biphasic cartilage layers. *J. Biomechanics*, 1994, **27**(11), 1347–1360.

39 **Kelkar, R.** and **Ateshian, G. A.** Contact creep of biphasic cartilage layers. *Trans. ASME, J. Appl. Mechanics*, 1999, **66**(1), 137–145.

40 **Soltz, M. A.** and **Ateshian, G. A.** A conewise linear elasticity mixture model for the analysis of tension–compression nonlinearity in articular cartilage. *Trans. ASME, J. Biomech. Engng*, 2000, **122**(6), 576–586.

41 **Krishnan, R., Park, S., Eckstein, F.,** and **Ateshian, G. A.** Inhomogeneous cartilage properties enhance superficial interstitial fluid support and frictional properties, but do not provide a homogeneous state of stress. *Trans. ASME, J. Biomech. Engng*, 2003, **125**(5), 569–577.